ANTIOXIDANTS & REDOX SIGNALING
Volume 14, Number 3, 2011

DOI: 10.1089/ars.2010.3302

Knockouts of SOD1 and GPX1 Exert Different Impacts on Murine Islet Function and Pancreatic Integrity

Xiaodan Wang,[1,*] Marko Z. Vatamaniuk,[1,*] Carol A. Roneker,[1] Matthew P. Pepper,[1] Liangbiao G. Hu,[2] Rebecca A. Simmons,[3] and Xin Gen Lei[1]

Abstract

Metabolic subtlety and clinical relevance of different forms of reactive oxygen species in diabetes remain unclear. Using single knockout of Cu,Zn-superoxide dismutase ($SOD1^{-/-}$) or Se-glutathione peroxidase-1 ($GPX1^{-/-}$) and their double-knockout (DKO) mouse models, we determined if elevating endogenously-derived superoxide and hydroperoxide exerted distinct impacts and mechanisms on body glucose homeostasis. Whereas the three knockout groups displayed decreased plasma insulin concentrations and islet β-cells mass, only $SOD1^{-/-}$ showed decreased body weight, increased blood glucose, and blocked glucose-stimulated insulin secretion. Null of SOD1 and GPX1 elevated respective islet superoxide and hydroperoxide production, and upregulated p53 phosphorylation. Knockout of SOD1 downregulated the foxhead box A2/pancreatic and duodenal homeobox 1 pathway in a superoxide-dependent fashion at epigenetic, mRNA, and protein levels in islets, but improved insulin signaling in liver and muscle. The $SOD1^{-/-}$ mice showed more apparent pancreatitis than the $GPX1^{-/-}$ mice that were more susceptible to the cerulein-induced amylase increase. Knockout of SOD1 impaired islet function, pancreas integrity, and body glucose homeostasis more than that of GPX1. Simultaneous ablation of both enzymes did not result in additive or aggravated metabolic outcomes. *Antioxid. Redox Signal.* 14, 391–401.

Introduction

Oxidative injury of pancreatic islet β-cells is implicated in diabetes and insulin resistance (38). Pancreatic β-cells are considered to be susceptible to oxidative stress because islets contain only 1% of catalase, 2% of Se-dependent glutathione peroxidase-1 (GPX1), and 29% of Cu,Zn-superoxide dismutase (SOD1) activities as in liver (29, 46). However, ectopic overexpression of these antioxidant enzymes *in vivo* has generated conflicting results. While a β-cell-specific overexpression of SOD1 enhanced mouse resistance to streptozotocin-induced diabetes (24), the same manipulation of catalase aggravated cytokine-induced and/or spontaneous type 1 diabetes in non-obese diabetic mice (30). Strikingly, a global overexpression of GPX1 induced type 2 diabetes-like phenotypes in full-fed mice (33) and chronic hyperinsulinemia in diet-restricted mice (48). Comparatively, diminishing superoxide by elevated SOD1 resulted in an opposite metabolic outcome from that by enhancing hydroperoxide-scavengers catalase and GPX1. Seemingly, these two forms of reactive oxygen species (ROS) may exert distinct effects on islet physiology and glucose homeostasis. Because that type of metabolic subtlety and its clinical relevance have not been thoroughly investigated, an apparent question arises as if and how knockouts of superoxide scavenger SOD1 and hydroperoxide scavenger GPX1 alone or together impact islets integrity and function.

The transcriptional factor pancreatic duodenal homeobox-1 (Pdx1) plays a pivotal role in β-cell growth and insulin synthesis (2, 43). As one of the key upstream regulators of Pdx1, forkhead box A2 (Foxa2) activates its gene expression *in vivo* (16, 27). Uncoupling protein-2 (Ucp2) is one of the key regulators of glucose-stimulated insulin secretion (GSIS) (49). As a main determinant of β-cell mass (5), apoptosis of islet β-cells can be triggered by the p53 phosphorylation (4). Consistent with other studies (6, 23), our previous study has shown an upregulation of Pdx1 and downregulation of Ucp2 in the GPX1-overproduced islets (48). However, little is known how these key regulators respond to elevation of *endogenously-derived* superoxide and hydrogen peroxide in islets.

The GPX1 overexpression-induced insulin resistance was associated with an attenuated phosphorylation of insulin

[1]Department of Animal Science, Cornell University, Ithaca, New York.
[2]Pfizer Global Research and Development, Pfizer, Inc. Chesterfield, Missouri.
[3]Department of Pediatrics, Children's Hospital Philadelphia and University of Pennsylvania, Philadelphia, Pennsylvania.
*These authors contributed equally to this work.

receptor (IR, β subunit) and protein kinase B (AKT, at Ser-473 and Thr-308) in liver and muscle (33). Presumably, the overproduced GPX1 enzyme diminished H_2O_2 and thereby its oxidative inhibition of protein tyrosine phosphatase activity (14, 31). It is unclear if elevating intracellular hydroperoxide and superoxide by knocking out of GPX1 and SOD1 alone or together produces a reciprocal outcome. Although ROS is implicated in pancreatitis (40) and antioxidants intake were linked to the risk or severity of pancreatitis (41), no study has explored the specific impact or mechanism of superoxide and hydrogen peroxide or their pertaining scavengers on pancreatitis.

To our best knowledge, there is no ideal chemical method to alter intracellular superoxide and hydrogen peroxide production specifically *in vivo* without complications. Because results from the GPX1 or SOD1 overexpressing mice may illustrate a more pharmacological rather than a physiological scenario, we have applied $SOD1^{-/-}$, $GPX1^{-/-}$, and their double-knockout (DKO) mouse models to determine if elevating the endogenously-derived superoxide and hydroperoxide exerted distinct impacts and unique mechanism on islet physiology, pancreatic integrity, and body glucose homeostasis. Our results reveal that the elevated intracellular superoxide in $SOD1^{-/-}$ mice exacerbated type 1 diabetes-like phenotype with a potent inhibition of the Foxa2/Pdx1-dependent pathway than those of hydroperoxide in $GPX1^{-/-}$ mice. This finding provides the first direct evidence for the peculiar functions and mechanisms of the two major forms of ROS and their scavenge enzymes in the development of pancreatitis and diabetes-like phenotypes.

Material and Methods

Mouse models, animal care, and in vivo *experiments*

The protocols for all mouse experiments were approved by the Institutional Animal Care and Use Committee at Cornell University. The $GPX1^{-/-}$, $SOD1^{-/-}$, and DKO mice were derived from the C57BL/6 line and the targeted specific knockouts were verified (28). All experimental mice were 3–6-month-old males unless other specified. Mice were given free access to a Torula yeast and sucrose-based diet (0.3 mg Se/kg) and distilled water (48). Mice were reared in plastic cages in a room with constant temperature (22°C) and a 12-h light-dark cycle. Tests with individual mice (fasted for 8 h, overnight) were conducted for blood glucose concentration, plasma insulin concentration, insulin tolerance (0.5 U/ kg; Humulin R; Eli Lilly, Indianapolis, IN), glucose tolerance (1 g/kg, D-glucose), and GSIS (1 g/kg), as described previously (48). To induce acute pancreatitis, mice (3 months of age, $n = 4$–6/genotype) were given an i.p. injection of cerulein at a dose of 50 mg/kg. Tail blood samples were collected at 0, 3, and 7 h after the injection to assay for serum amylase activity.

Histology and immunohistochemistry of pancreas

Quantification of β-cell mass in four genotypes was performed using immunostaining of pancreatic sections ($n = 4$ mice x 3 slides per genotype) with a guinea pig polyclonal antibody against mouse insulin (Zymed, San Francisco, CA) as described previously (48). For diagnosis of pancreatitis, pancreas tissue sections from the four genotypes (2- and 14-months of age, $n = 4$ mice per genotype by age) were stained with hematoxylin and eosin, and the slides were examined by a board-certified pathologist (LGH). To determine if the increased intracellular superoxide in the $SOD1^{-/-}$ mice quenched NO to form peroxynitrite in pancreas, nitrotyrosine formation, an *in vivo* indicator of peroxynitrite activity (17) was compared between the WT and $SOD1^{-/-}$ as previously described (50). The PBS-treated WT and the acetaminophen-treated GPX1 overexpressing mice were used as negative and positive controls, respectively (50).

In vitro *experiments*

Detailed protocols, reagents, and instruments for islet isolation, culture, insulin secretion, and intracellular total ROS production were the same as described before (48). For the test of ATP production, isolated islets (50 per sample, $n = 3$ per genotype by treatment) were cultured in RPMI medium for 2 h, pre-conditioned in Krebs–Ringer bicarbonate buffer for 90 min, and then incubated for 60 min with 4 or 30 m*M* glucose in the same buffer. The ATP was extracted from islets and assayed in triplicates using a kit (Enliten ATP assay kits, Promega, Madison, WI). For the test of intracellular superoxide, islets (100 per sample, $n = 4$ per genotype by treatment) were cultured in the RPMI 1640 media and were loaded with the MitoSOX Red superoxide indicator (1 μg/ ml), (Molecular Probes, Eugene, OR) for 30 min (44). The islets were also incubated with the medium only (basal), hypoxanthine/ xanthine oxidase (HX/XO, superoxide generator: 1 μM/500 units/L), diethyldithiocarbamate (DETC, a potent SOD inhibitor, 1 m*M*) or copper diisopropylsalicylate (CuDIPS, a potent SOD mimic, 2 μM) for 24 h.

Three *in vitro* experiments were conducted to determine whether the suppressed Foxa2 protein levels in the $SOD1^{-/-}$ islets were caused by the diminished superoxide-scavenging capacity. Islets isolated from four WT, $SOD1^{-/-}$, and $GPX1^{-/-}$ mice each were pooled and divided into three or two groups (200 islets per sample, $n = 3$ per treatment). The treatments of islets included: 1) medium only (10 m*M* glucose and 10% fetal bovine serum); 2) DETC; 3) HX/XO; and 4) CuDIPS. Concentrations of the three compounds/systems were the same as described above. After 24 h of incubation, islets were collected to assay for Foxa2 protein as described below.

Quantification of mRNA, protein, epigenetic modifications, and activator binding of pdx1

Total RNA of islets (200 per sample, $n = 6$ mice per genotype) was prepared (48) to determine insulin-related gene expression using real time Q-PCR. Primer sequences for tested genes are described in Supplemental Table 1 (*see* www .liebertonline.com/ars). Determinations of acetylation of histone 3 (H3), tri-methylation of H3lysine 4 (H3K4), and Foxa2 protein binding in the proximal 5'promoter region of the *pdx1* were conducted as previously described (36). Total protein or phosphor-protein amounts of insulin-related signal molecules, GPX1, and SOD1 in homogenates of pancreas, liver, muscle ($n = 6$–8 per genotype), and islets (400 per sample, $n = 4$ mice per genotype) were determined as previously described (33, 48). The homogenates (20–50 μg protein) were resolved by SDS-polyacrylamide gel (12%) electrophoresis. Antibodies are listed in Supplemental Table 2 (*see* www .liebertonline.com/ars).

Statistical analyses

Quantitative data were analyzed using SAS (release 6.11; SAS Institute, Cary, NC). Genotype or treatment effects were tested by one or two-way ANOVA and Student's t test. Data are presented as mean ± SE and significance was set at $p \leq 0.05$.

Results

Knockout of GPX1 and SOD1 produced different metabolic phenotypes

Knockouts of SOD1 and GPX1 proteins in the respective genotypes were confirmed (Fig. 1a). Body weights of SOD1$^{-/-}$ mice at and after 4 months of age were lower ($p \leq 0.05$) than those of WT (Fig. 1b). Fasting blood glucose concentrations were elevated in all three knockout groups compared with WT, but only the SOD1$^{-/-}$ mice reached statistical significance (Fig. 1c). Starting at 3 months of age, fasting plasma insulin concentration (postmortem heart blood) became approximately 50% lower ($p < 0.05$) in SOD1$^{-/-}$ and GPX1$^{-/-}$ than that of WT, with further reduction ($p \leq 0.05$) in the DKO mice (Fig. 1d). Monthly glucose tolerance test indicated more efficient blood glucose clearance at 4 months of age ($p < 0.05$) in the SOD1$^{-/-}$ and DKO (at 15 and 30 min) mice, as compare to WT (Fig.1e). Monthly insulin tolerance test showed improved insulin sensitivity ($p < 0.05$) at 4 months of age in the SOD1$^{-/-}$ and DKO mice than in the WT mice (Fig.1f). Overall, the DKO mice exhibited phenotypes similar to those SOD1$^{-/-}$, but different from those of GPX1$^{-/-}$.

Knockout of SOD1 impaired islet physiology more than that of GPX1

The GSIS was attenuated ($p \leq 0.05$) in the GPX1$^{-/-}$ than WT mice, and was virtually blocked in the SOD1$^{-/-}$ and DKO mice (Fig. 2a). The same genotype differences in GSIS were also shown in isolated islets (Fig. 2b). Because GSIS in islets depends on ATP production (32), we measured ATP levels of

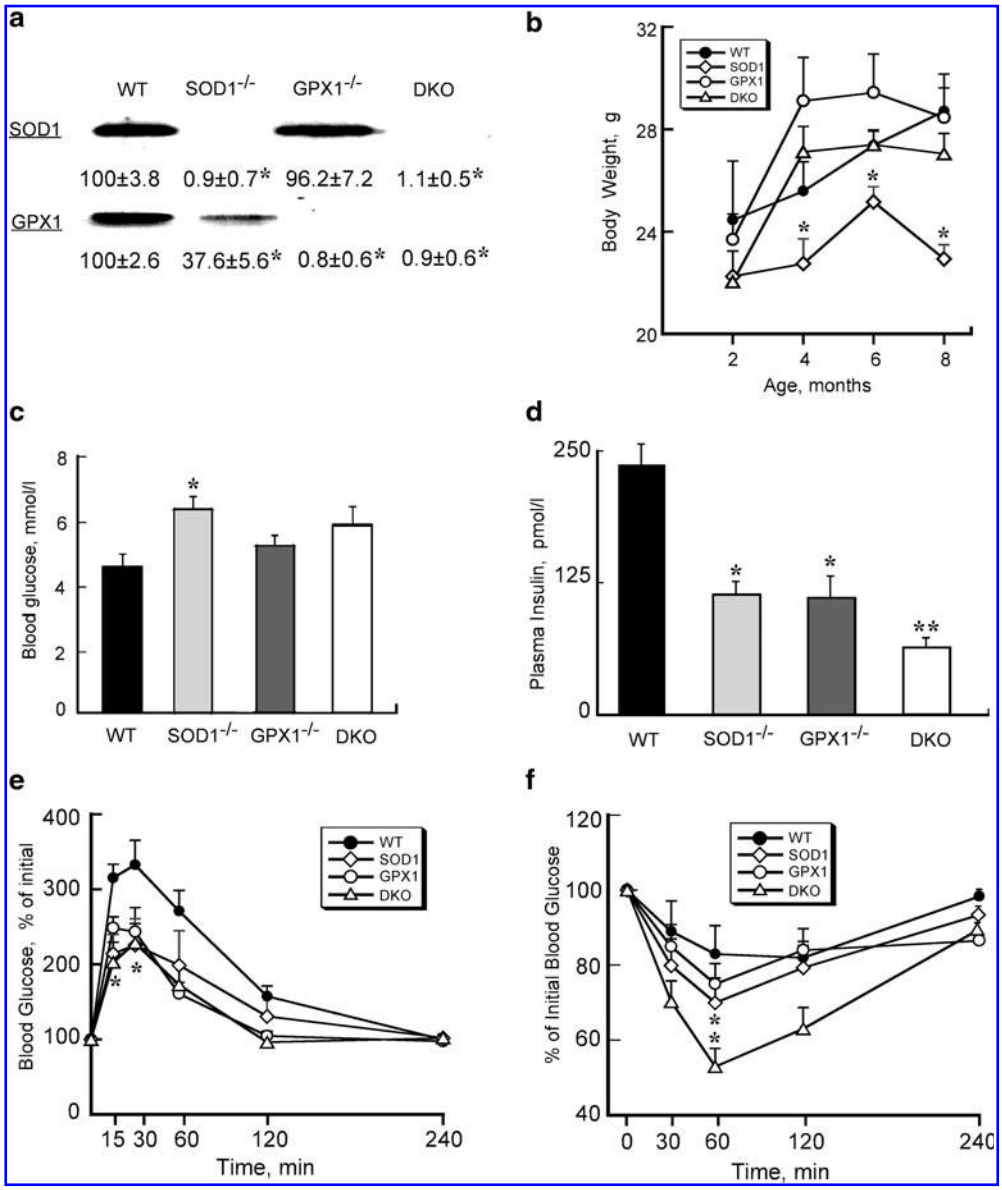

FIG. 1. Altered glucose homeostasis phenotypes in SOD1$^{-/-}$, GPX1$^{-/-}$, and DKO mice. (**a**) Verification of respective protein knockout in islets of SOD1$^{-/-}$, GPX1$^{-/-}$, and DKO mice by Western blot analysis. (**b**) Body weights of the four genotypes from 2 to 6 months of age. (**c**) Fasting blood glucose concentrations of the four genotypes at 3 months of age. (**d**) Fasting plasma (postmortem heart blood) insulin concentrations of the four genotypes at 3 months of age. (**e**) Glucose tolerance test at 4 months of age (GTT, 2 g/kg). (**f**): Insulin tolerance test at 4 months of age (ITT, 0.5 U/kg). All data are means ± SE ($n = 5$–6). *Asterisks* indicate differences ($p \leq 0.05$) from the WT. *Double asterisks* indicate differences ($p \leq 0.05$) from all other groups.

islets (Fig. 2c). Compared with the WT controls, islet ATP production was lower ($p < 0.05$) in all three knockout groups at the high glucose and also in the SOD1$^{-/-}$ group at the low glucose. As shown in Figure 2d, islet β-cell mass in pancreatic tissue was 41%–56% lower ($p < 0.05$) in the three knockout groups than that of the WT.

Knockout of SOD1 and GPX1 elevated respective islet superoxide and hydroperoxide production

To test if metabolic phenotypes of SOD1$^{-/-}$ and GPX1$^{-/-}$ were due to alterations of specific ROS, we determined intracellular peroxide (total ROS) and superoxide in cultured islets (Fig. 3a). The SOD1$^{-/-}$ and DKO islets exhibited higher level of total ROS (hydroperoxide and superoxide shown by the green fluorescence) at the basal glucose level than the WT. The high glucose-induced ROS production appeared strongest in the SOD1$^{-/-}$, followed by GPX1$^{-/-}$, DKO, and WT islets. The baseline and the induced (HX/XO) superoxide production in SOD1$^{-/-}$ and DKO islets were greater than in the WT (Fig. 3b). Treating the WT and GPX1$^{-/-}$ islets with the SOD inhibitor DETC elevated superoxide formation, while treating the SOD1$^{-/-}$ and DKO islets with the SOD mimic CuDIPS attenuated the superoxide production (Fig. 3c). These detected responses validated our measurement of islet superoxide, reflecting a potent impact of SOD1 knockout on islet superoxide tone. In comparison, the shift in intracellular ROS by the GPX1 knockout was moderate. The DKO showed similar ROS and superoxide profiles to those of SOD1$^{-/-}$. To test if the elevated superoxide in SOD1$^{-/-}$ islets quenched NO to form peroxynitrite (17), we stained pancreatic sections of WT and SOD1$^{-/-}$ with anti-nitrotyrosine antibody. Using liver sections from the acetaminophen-treated WT mice as a positive control (50), we did not detect any peroxynitrite staining in either genotype (Supplemental Fig. 1; *see* www.liebertonline.com/ars). Thus, their metabolic phenotypes could not be attributed to possible NO quenching in the SOD1$^{-/-}$ islets.

Knockout of SOD1 suppressed Foxa2/Pdx1 expression in a superoxide-dependent pathway

To explore molecular mechanisms for the islet phenotypes of the three knockout groups, we determined mRNA and

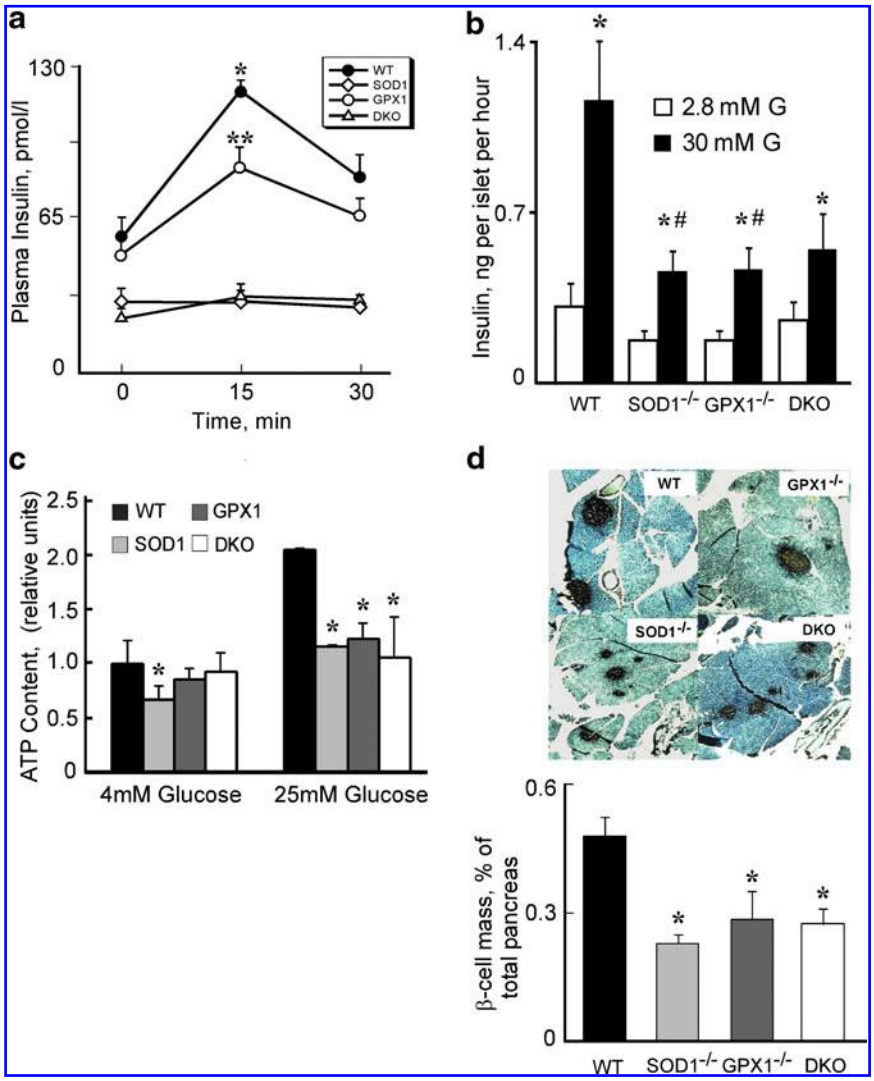

FIG. 2. Islets physiology of in SOD1$^{-/-}$, GPX1$^{-/-}$ and DKO mice. (**a**) Effects of knockouts of SOD1 and GPX1 on glucose-stimulated insulin secretion (GSIS, 1g/kg). (**b**) GSIS in cultured islets that (30 per sample) were incubated in 1 ml of Hanks buffered saline solution containing 2.8 (2.8 m*M* G) or 30 (30 m*M* G) mM glucose at 37°C for 1 h. (**c**) ATP content in cultured islets. (**d**) Representative images ($n = 3$ mice x three slides/genotype) of pancreatic β-cell mass shown by insulin staining (40X magnification) (*upper panel*) and quantification of β-cell mass (*lower panel*). Data represent mean ± SE; $n = 4$–6 for *panels a, b,* and *c*, and $n = 9$ for *panel d*. **Asterisks* indicate significant differences ($p < 0.05$) from the respective WT within the same treatment, # indicates the treatment effect within the genotype (*panel B*), and ** indicates that the GPX1$^{-/-}$ group was different ($p < 0.05$) from both WT and SOD1$^{-/-}$ and DKO groups (For interpretation of the references to color in this figure legend, the reader is referred to the web version of this article at www.liebertonline.com/ars).

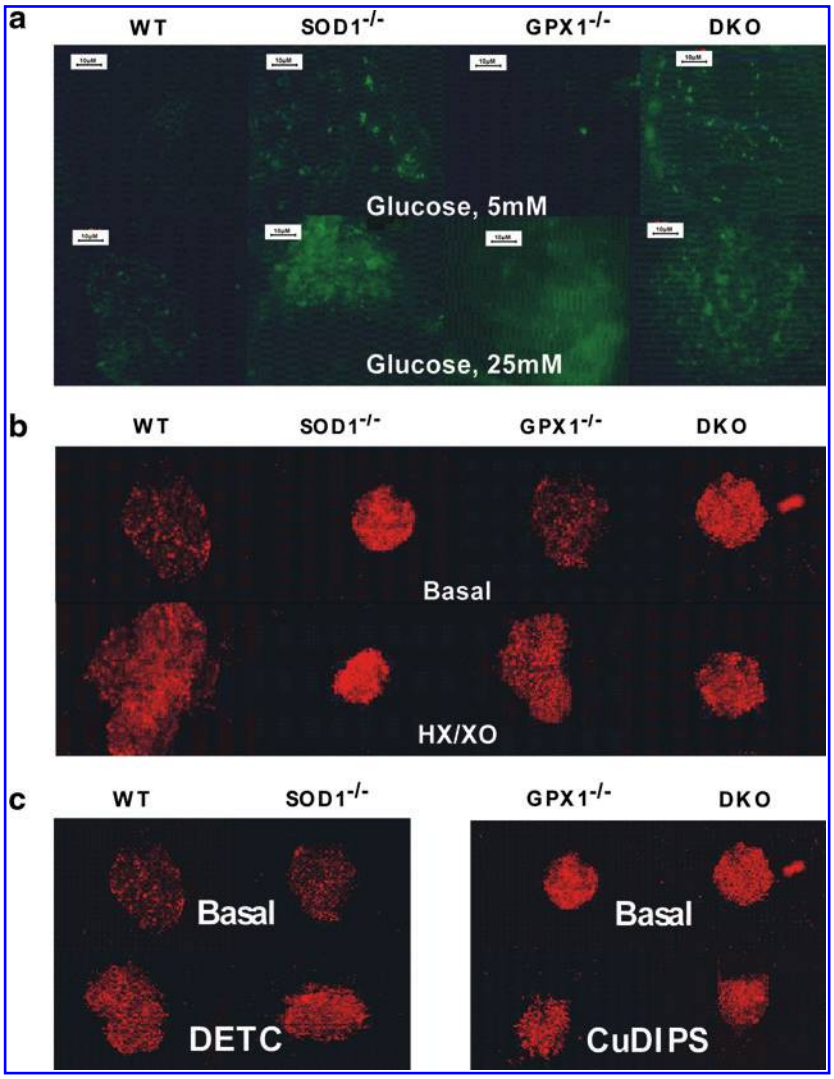

FIG. 3. Intracellular ROS Levels in SOD1$^{-/-}$, GPX1$^{-/-}$, and DKO mouse islets. (**a**) Islet peroxide levels (*green fluorescence*) after 5 h treatment with 5 m*M* and 25 m*M* glucose. (**b**) Islet superoxide levels (*red fluorescence*) after 5 h treatment without or with the superoxide generator: 200 μM HX and 50 mU/ml XO. (**c**) Islets superoxide levels after 5 h treatment with SOD1 inhibitor (100 μM DETC) and SOD1 mimic (10 μM CuDIPS). The images (40X magnification) shown were the representative of four sets of data (For interpretation of the references to color in this figure legend, the reader is referred to the web version of this article at www.liebertonline.com/ars).

protein expression of three important regulators (Foxa2, Pdx1, and Ucp2) of β-cell mass, insulin synthesis, and GSIS (8, 25, 26). Compared with WT, the mRNA and protein levels of Foxa2 and Pdx1 in SOD1$^{-/-}$ and DKO islets were approximately 45%–70% lower ($p < 0.05$, Figs. 4a and 4b). Knockout of GPX1 resulted in only a decrease ($p < 0.05$) of Pdx1 protein. The three knockout groups had decreased *preproinsulin1* mRNA and increased Ucp2 protein, but only the DKO group displayed elevated ($p < 0.05$) *ucp2* mRNA.

To verify if the downregulation of Foxa2 protein in the SOD1$^{-/-}$ and DKO islets was indeed caused by the loss of superoxide scavenging capacity, we treated islets of various genotypes with DETC, CuDIPS, and HX/XO (Fig. 4c). While DETC completely suppressed Foxa2 in the WT islets, CuDIPS restored the protein in the SOD1$^{-/-}$ islets to the WT level. Because treating the WT or GPX1$^{-/-}$ islets with HX/XO displayed little effect on the protein, the two genotypes had adequate SOD1 activity to cope with the accelerated superoxide generation. The low baseline level of Foxa2 in the SOD1$^{-/-}$ islets was further diminished by the treatment of HX/XO.

Because acetylation of histone 3 (H3) and trimethylation of H3K4 in the proximal 5′promoter region of *pdx1* are crucial for its transcription (36), we compared impacts of SOD1 and GPX1 null on these two events. Compared with the WT, the SOD1$^{-/-}$ and DKO islets displayed approximately 50% ($p < 0.05$) reduction in H3 acetylation (Fig. 5a) and H3K4 methylation (Fig. 5b) in the *pdx1* promoter region. Consistently, the Foxa2 binding to the *pdx1* promoter was decreased ($p < 0.05$) by 50% in the SOD1$^{-/-}$ and DKO groups (Fig. 5c). To further explore molecular mechanisms for the different phenotypes of SOD1$^{-/-}$ and GPX1$^{-/-}$, we screened another 12 insulin synthesis and secretion-related genes in the four genotypes (Supplemental Fig. 2; *see* www.liebertonline.com/ars). Consistent with the lowest islet insulin gene expression (Fig. 4a) and plasma insulin concentrations (Fig. 1d), the DKO islets also exhibited downregulated ($p < 0.05$) mRNA levels of *mafA*, *beta2*, and *hnf4α* that are the most important transcriptional factors of β-cell growth and insulin synthesis (11, 19). Five GSIS-related genes (*glut2*, *kir6.2*, *irs2*, and *glpr1*) (3, 21, 45) were downregulated ($p < 0.05$) in the SOD1$^{-/-}$ and DKO islets, which might help explain the blocked GSIS *in vivo* and *in vitro*. The SOD1$^{-/-}$ and DKO islets had upregulated ($p < 0.05$) *preproglucagon*, *glucokinase*, and (or) *cFos* (redox-sensitive) compared with WT.

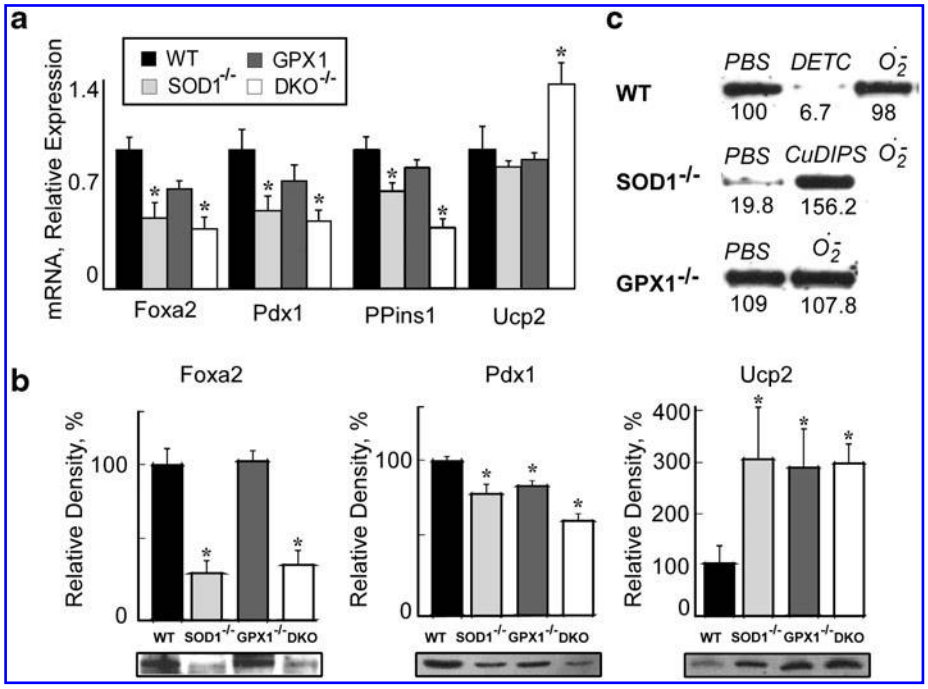

FIG. 4. Changes in gene and protein expressions of key regulators in SOD1$^{-/-}$, GPX1$^{-/-}$, and DKO mice. (**a**) Real time Q-PCR analysis of Foxa2, Pdx1, preproinsulin 1 (PPins1), and Ucp2 mRNA in islets (200 per sample/animal, $n=6$ mice/genotype). Data are means ± SE ($n=6$). *Asterisks* indicate differences from WT ($p<0.05$). (**b**) Western blot analysis of Foxa2, Pdx1, and Ucp2 proteins in pancreas of the four genotypes. *Lower panel*: representative ($n=4$) immunoblots of the three proteins separated by SDS-polyacrylamide gel (12%) electrophoresis (20–50 g protein/lane). *Upper panel*: the relative density of the protein bands quantified using the Alpha-Imager 2200 system (Alpha Innotech, San Leandro, CA), and normalized to that of ß-actin on the same membrane. Values are expressed as mean ± SE ($n=4$), and the *asterisk* * indicates difference ($p<0.05$) from the WT. (**c**) Western blot analysis of Foxa2 protein in islets ($n=200$ per sample, $n=$ three/treatment) in response to 1 m*M* DETC (a potent SOD inhibitor), 2 μM CuDIPS (a potent SOD mimic), or 1 μM–500 μU/ml HX/XO (superoxide generator). The values ($n=3$) under the image represent the relative Foxa2 protein levels.

Islet p53 was activated by null of SOD1 and GPX1

To determine if apoptosis was involved in the decreased β-cell mass of the three knockout groups, we assayed islet p53 phosphorylation (ser-15) (Fig. 6). With similar total p53 protein among the four genotypes, the SOD1$^{-/-}$ and GPX1$^{-/-}$ group had 1.4-fold higher ($p<0.05$) of P53^{ser15} than the WT. Notably, the DKO islets showed no substantial change in P53^{ser15} over the WT. To link the activation of p53 to the presumed increased oxidative stress in the islets, we determined phosphor-p38 MAPK, a member of the MAP kinase family involved in cytokine-induced β-cell apoptosis (39). Compared with WT, the three knockout groups had greater ($p<0.05$) amount of phosphor-p38 MAPK. Likely, an unbalanced production or shift of superoxide and hydroperoxide, rather than the total ROS, activated the p53-dependent apoptotic pathway.

Knockout of sod1 improved insulin signaling in liver and muscle

To explain the improved insulin sensitivity in the SOD1$^{-/-}$ and DKO mice (at 4 months of age), we determined total and phosphorylated IR (β subunit), insulin substrate 1 (IRS-1), and AKT in two primary target tissues of insulin: liver and muscle of mice. Compared with WT, knockout of SOD1 and GPX1 alone or in combination elevated phosphorylation of AKT (both AKT^{ser473} and AKT^{thr308}) by 35 to 78% ($p<0.05$) (Fig. 7a) in muscle. Meanwhile, total protein of hepatic IR (β unit) was 35 and 18% greater ($p<0.05$) in the SOD1$^{-/-}$ and DKO mice than the WT, respectively (Fig. 7b). These two changes in the SOD1$^{-/-}$ and DKO might additively help improve their body insulin sensitivity to adapt to the diminished insulin production. The upregulation of only AKT phosphorylation in the GPX1$^{-/-}$ mice might be insufficient to produce a significant functional improvement.

Knockout of SOD1 and GPX1 rendered mice different susceptibility to pancreatitis

To determine if null of SOD1 and GPX1 exerted different impacts on the exocrine integrity of pancreas, we conducted histological analyses of pancreas from 2- and 14-month-old mice. The WT pancreas remained normal at both ages (Figs. 8a and 8b), while the GPX1$^{-/-}$ pancreas showed minimal focal chronic pancreatitis along with minimal hypertrophy of islet β-cells at 2 months of age. The 14-month-old GPX1$^{-/-}$ mice remained focal pancreatitis with moderate acinar hypertrophy and slight interstitial mononucleated cell infiltration. The 2-month-old SOD1$^{-/-}$ mice displayed focally extensive interstitial pancreatitis along with acinar cell degeneration and necrosis. The old SOD1$^{-/-}$ mice developed multiple nodular acinar hypertrophy, fibrosis, lobular, severe with loss of islet, and islet cells containing eosinophilic granules and hypertrophic. The young DKO mice showed minimal, but multifocal interstitial pancreatitis; and the old DKO mice had mild islet cell hypertrophy mixed with eosinophilic granule-laden cells. After an i.p. injection of cerulein (15), all four genotypes (3-months-old) developed mild pancreatitis at 7 h (data not shown). However, the SOD1$^{-/-}$ and DKO mice exhibited lower ($p<0.05$) whereas the GPX1$^{-/-}$ mice had greater ($p<0.05$) increase in serum amylase activity (an indicator of acute pancreatitis) than the WT (Fig. 8b). This difference between the SOD1$^{-/-}$ and GPX1$^{-/-}$ mice depicted another distinct impact of superoxide and hydroperoxide in pancreas.

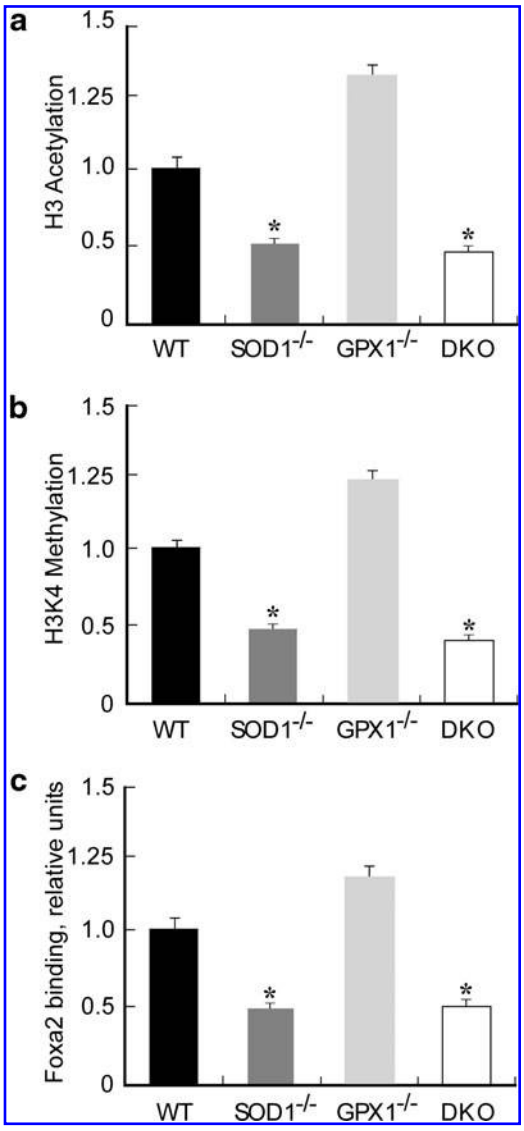

FIG. 5. Epigenetic modifications of *pdx1* promoter and its binding to Foxa2 in SOD1$^{-/-}$, GPX1$^{-/-}$, and DKO islets. Immunoprecipitation was carried out overnight with preimmune serum (negative control) or primary antibodies (all from Upstate Biotech/Millipore) to the acetylated histone 3 (H3) and trimethyl-histone 3 lysine 4 (H3K4). After protein elusion, the released DNA was extracted, precipitated, and resuspended in water. DNA sequences in the "input" and the immunoprecipitated samples were quantified relative to the WT by real-time Q-PCR. (**a**) H3 acetylation in the *pdx1* promoter region. (**b**) H3K4 trimethylation in the *pdx1* promoter region. (**c**) Binding of Foxa2 to the *pdx1* promoter. The values are mean ± SE ($n = 4$) and expressed as relative to the WT. The *asterisks** indicate difference ($p < 0.05$) from the WT.

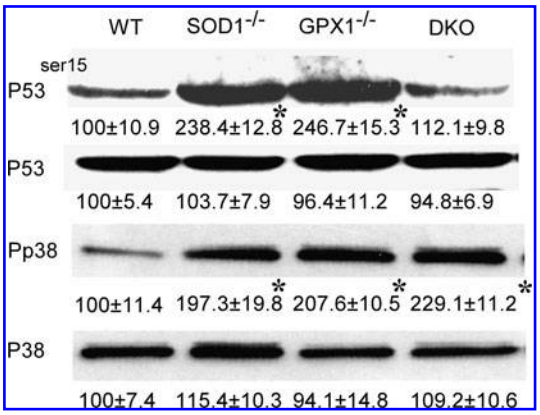

FIG. 6. Effects of knockouts of SOD1 and GPX1 on total and phosphorylated protein of p53 (P53 and P53^{ser15}) and p38 MAPK (P38 or Pp38) in islets ($n = 200$ per sample). Blots are representative images of three independent analyses, and values under respective bands are relative density (mean SE, $n = 3$). The *asterisks** indicate difference ($p < 0.05$) from the WT.

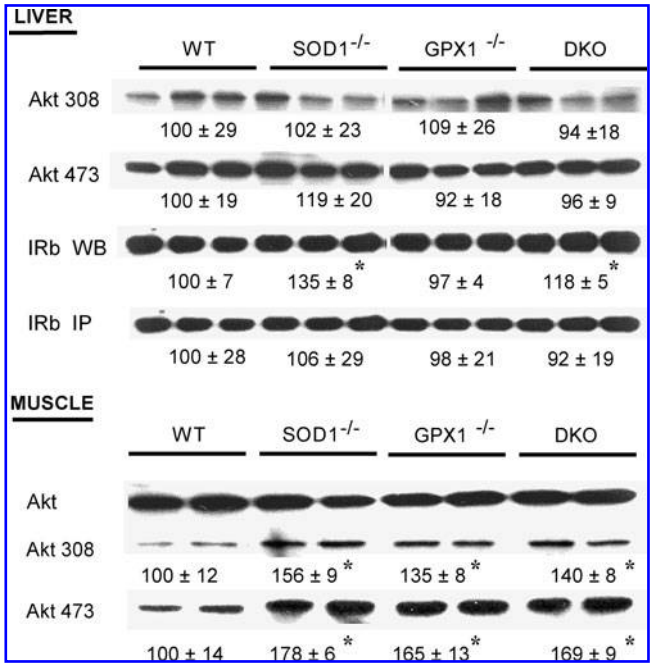

FIG. 7. Impacts of knockouts of SOD1 and GPX1 on liver and muscle insulin signaling. For determining total (WB) and phosphorylation (IP) of hepatic insulin receptor (β-subunit, IR$_\beta$ IP), mice ($n = 6$) fasted overnight (8 h) were given an ip injection of insulin (5 U/kg) and killed to collect liver 3 min after the injection. After homogenization and immunoprecipiation with the anti-IR$_\beta$ antibody, the precipitates were subjected to Western blot analysis using an antibody against phosphotyrosine (4G10). For determining Akt protein and phosphorylation (Thr308 and Ser473), liver and soleus muscle samples were collected 8 min after mice (fasted overnight for 8 h, $n = 6$) were given an ip injection of insulin (10 U/kg). For a given protein, the *upper panel* shows the representative images of six independent analyses, and the *lower panel* shows the relative density of protein bands (mean ± SE, $n = 6$). The *asterisks** indicate difference ($p < 0.05$) from the WT.

Discussion

Roles of superoxide vs. hydroperoxide in glucose homeostasis and islet physiology

The most striking finding of present study is that knockout of SOD1 produced severer metabolic phenotypes of islet and glucose metabolism abnormality than that of GPX1. Compared with liver, islets have moderately low SOD1 activity

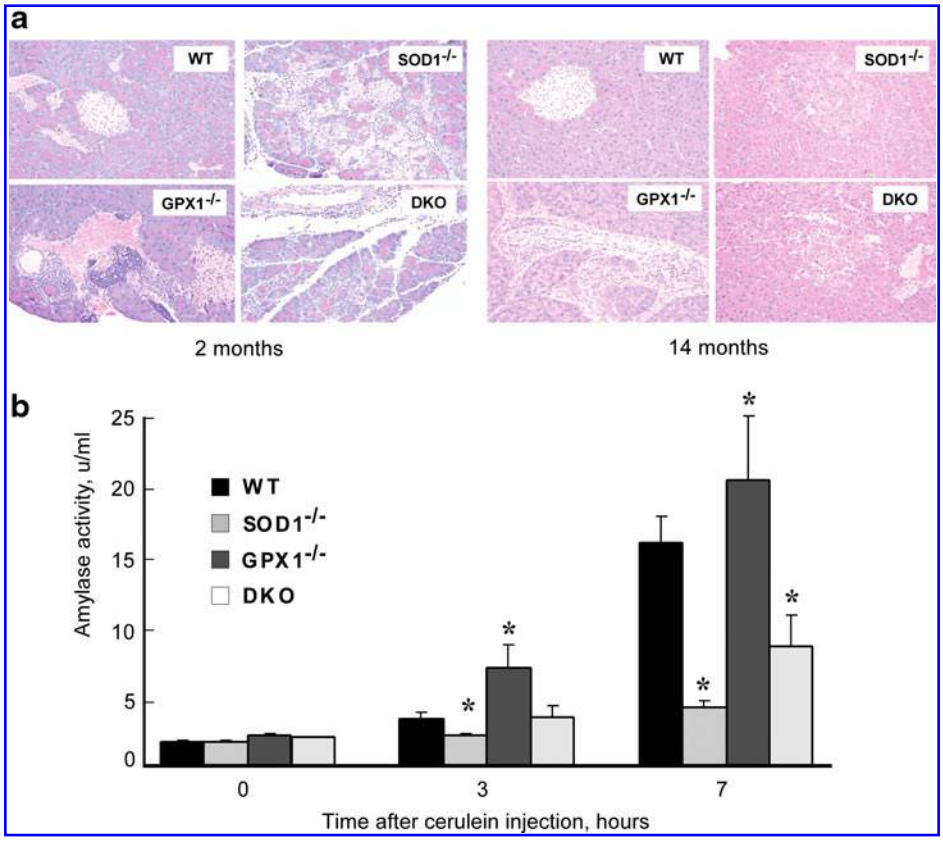

FIG. 8. Impacts of knockouts of SOD1 and GPX1 on pancreatic integrity and cerulein-induced amylase release. (**a**) Representative images ($n = 4$ mice x three slides per genotype by age) of pancreatic sections stained with hematoxylin and eosin (40X magnification). *Left panel* (2 months of age): WT, normal structures of insulin secreting islet, interstitial blood vessels and acini; $GPX1^{-/-}$, multifocal interstitial infiltration of lymphocytes and macrophages; $SOD1^{-/-}$, necrotizing pancreatitis, focally extensive; DKO, interstitial pancreatitis with individual acinar cell degeneration and necrosis. *Right panel* (14 months of age): WT, normal structures of insulin secreting islet and exocrine acinus; $GPX1^{-/-}$, perivascular and interstitial infiltration of neutrophils, macrophages and lymphocytes; $SOD1^{-/-}$, focal acinar nodular hyperplasia; DKO, interstitial pancreatitis with minimal acinar cell degeneration. (**b**) Cerulein-induced amylase release in plasma. Mice (3 months of age, $n = 4$–6/genotype) were given an ip injection of cerulein at dose of 50 mg/kg. Tail blood samples were collected at 0, 3, and 7 h after the injection for the assay of serum amylase activity. Values are mean ± SE ($n = 4$–6). The *asterisks** indicate difference ($p < 0.05$) from the WT (For interpretation of the references to color in this figure legend, the reader is referred to the web version of this article at www.liebertonline.com/ars).

(only 24%) and extremely low (only 1%) of GPX1 activity (46). It is somewhat surprising that knockout of these two enzymes actually elevated intracellular levels of their respective ROS substrates: superoxide and hydroperoxide. However, the increased superoxide in the $SOD1^{-/-}$ islets did not quench nitric oxide (34). Because the DKO mice shared phenotypes similar to those of $SOD1^{-/-}$ mice that were featured with greater changes in body weight, hyperglycemia, GTT, ITT, and GSIS than those of the $GPX1^{-/-}$ mice, altering intracellular superoxide disturbed islet function and body glucose metabolism more than that of hydroperoxide. To our best knowledge, this represents the first direct evidence for such unique features of these two forms of ROS in physiological conditions. Although originations and reactivity of superoxide and hydroperoxide are different (13), their metabolic subtlety in β-cell dysfunction and diabetes has been ignored (22). Our finding highlights the importance in *concretizing* ROS regulations of islet function and glucose metabolism, and helps explain why overexpressing superoxide and hydroperoxide scavenging enzymes produced variable or opposite outcomes (24, 30, 33). Clinically, our results provide new clues to deliver target treatment of particular disorders of diabetes associated with specific forms of ROS. An excellent example is that treating diabetic renal injury of obese rats with the SOD1 mimetic (tempol) only attenuated pathogenesis of inflammation, proliferation, and fibrotic changes caused by superoxide, but showed no effect on the H_2O_2-associated glomerular hemodynamics and proteinuria (37). Cardiac overexpression of catalase rescues cardiac contractile dysfunction induced by insulin resistance (12), while combined administrations of SOD1 and catalase mimics offered better treatment effects of diabetic complications than the sole use of SOD1 mimic (9).

Distinct mechanisms by SOD1 and GPX1 on insulin synthesis, secretion, and function

While knockout of SOD1 and GPX1 produced similar decreases in pancreatic β-cell mass and plasma insulin concentration, responses of key regulators of these parameters in the two genotypes were different. The Foxa2 mRNA, protein, and its binding to the *pdx1* promoter were downregulated in the $SOD1^{-/-}$ islets, but showed no change in the $GPX1^{-/-}$ islets. More convincingly, a direct link between Foxa2 and the SOD1 was established by the diminishing of Foxa2 in the WT islets treated with the SOD inhibitor, and the restoration of the protein in the $SOD1^{-/-}$ islets treated with the SOD mimic. Reciprocally, the SOD1 promoter contains four consensus Pha-4/Foxa binding sites (35), and the mouse *sod1* is a transcriptional target of Foxa1 (7). The decreased Pdx1 protein in the $SOD1^{-/-}$ islets was certainly involved in the islet gene transcription because the *pdx1* mRNA, along with the H3 acetylation and H3K4 methylation in the *pdx1* promoter region (36), was downregulated.

Without similar declines in *pdx1* mRNA and epigenetic modifications in the GPX1$^{-/-}$ islets, the decreased Pdx1 protein was probably attributed to an attenuated protein translation and(or) accelerated protein phosphorylation and degradation by the elevated H_2O_2 (6). In addition, the SOD1 knockout produced stronger impact on *mafA* mRNA than the GPX1 knockout, despite similar effects on islet *hnf4α* and *beta2* mRNA. Because the islet p53-dependent apoptotic signaling did not fully match decrease of pancreatic islet β-cell mass across all three knockout groups, it remains to be clarified whether apoptosis contributed to that change. Future research should also be conducted to illustrate how the changes of Pdx1 and Foxa2 induced by knockout of GPX1 and SOD1 affect β-cell differentiation, survival, and regeneration.

The similar decreases in ATP production and increases in Ucp2 protein in the SOD1$^{-/-}$ and GPX1$^{-/-}$ mice were consistent with their attenuated GSIS *in vivo* and (or) *in vitro* as compared with the WT. The upregulation of Ucp2 protein in the absence of SOD1 and GPX1 might constitute a compensatory mechanism to uncouple the mitochondrial and prevent further ROS formation (48). The concurrent downregulation of *glut2*, *kir6.2*, and *glpr1* expressions in the SOD1$^{-/-}$ and DKO islets further explains why *in vivo* and *in vitro* GSIS were virtually blocked in these two genotypes. These three molecules are important regulators of GSIS, and their alteration or modification has been involved in insulin secretion disorders (3, 42, 45). It is scientifically fascinating and clinically relevant for us to illustrate such a distinct impact of superoxide and hydroperoxide on their gene expression.

Knockout of SOD1 enhanced AKT phosphorylation in muscle and total amount of IR (β unit) in liver, which might jointly help improve insulin sensitivity over the WT. In contrast, knockout of GPX1 elevated only AKT phosphorylation in muscle and resulted in no substantial improvement in body insulin sensitivity. Previous studies have provided evidence that SOD3 gene polymorphism is associated with insulin resistance and incidence of diabetes (1). However, elevating GPX1 activity has been shown to be associated with insulin resistance in mice (33) or humans (10). In fact, H_2O_2 inhibits protein tyrosine phosphatase (e.g., PTP-1b) activity (31), and thereby prolongs insulin-induced phosphorylation of insulin receptor β-subunit (18) and AKT (14). Thus, certain amounts of intracellular hydroperoxide are required for sensitizing insulin signaling. The improved insulin sensitivity in the SOD1$^{-/-}$ mice implies an inhibition of protein tyrosine phosphatases by superoxide similar to or stronger than that by H_2O_2. That improvement could in part signify an adaptation to the diminished insulin production and secretion. However, the observed differences in body weight and yet to be determined differences in body composition (fat and lean mass), organ development, and feed intake among the three knockout groups might also be associated with their insulin sensitivity.

Net metabolic effects of double knockout of GPX1 and SOD1 resemble those of SOD1 knockout in all of the tested molecular mechanisms except for p53 phosphorylation. Thus, all these mechanisms were mainly controlled by changes of intracellular superoxide instead of H_2O_2 levels. The lack of upregulation of p53 phosphorylation in the DKO islets, contrary to the single null groups, implies that the balance between SOD1 and GPX1 for maintaining appropriate ratio of superoxide and hydrogen peroxide regulates islet apoptosis.

Pathological implications of sod1 and gpx1 knockout models

Compared with WT, the SOD1$^{-/-}$ mice developed type 1 diabetes-like phenotype. The signs included decreased body weight and β-cell mass, hypoinsulinemia, diminished GSIS, and hyperglycemia. The improved glucose tolerance and increased insulin sensitivity might compensate and thus help delay or escape the onset of overt symptoms. However, these mice had elevated blood ketone bodies and urine glucose (data not shown), increased bone deterioration (47), and eye problems (20) similar to the long-term complications of type 1 diabetes. It seems that these SOD1$^{-/-}$ mice may serve as a novel model to study ROS-related type 1 diabetes and its complications. Compared with the SOD1$^{-/-}$ mice, the GPX1$^{-/-}$ mice developed only moderate hyperglycemia and showed no body weight change over the WT. However, these GPX1$^{-/-}$ mice were sensitive to the cerulein-induced increase in serum amylase and thus may serve as a model for studying role of ROS and antioxidants in acute pancreatitis.

Overall, our study reveals that knockout of SOD1 impaired islet function, pancreas integrity, and body glucose homeostasis more than that of GPX1. However, caution should be given for interpretation of this novel finding. Because all three global knockout models developed pancreatitis, their metabolic phenotypes are likely associated with inflammation and potential impairments of both endocrine and exocrine functions (40, 41). Impacts of GPX1 and SOD1 knockouts on cytokine gene expression and function in islets and pancreas should be monitored in future research. More importantly, β-cell specific knockout models of SOD1 and GPX1 should be generated to elucidate metabolic roles of these enzymes specifically in β-cell integrity and function.

Acknowledgments

The authors thank Drs. O. Vatamaniuk and Q. Long for the use of microscope facilities. This work was supported in part by National Institutes of Health Grants DK53018 (XGL) and DK55704 (RAS).

Author Disclosure Statement

The authors declare that no competing financial interests exist.

References

1. Adachi T, Inoue M, Hara H, Maehata E, and Suzuki S. Relationship of plasma extracellular-superoxide dismutase level with insulin resistance in type 2 diabetic patients. *J Endocrinol* 181: 413–417, 2004.
2. Ahlgren U, Jonsson J, Jonsson L, Simu K, and Edlund H. Beta cell-specific inactivation of the mouse Ipf1/Pdx1 gene results in loss of the beta-cell phenotype and maturity onset diabetes. *Genes Dev* 12: 1763–1768, 1998.
3. Ahren B. Islet G protein-coupled receptors as potential targets for treatment of type 2 diabetes. *Nat Rev Drug Discov* 8: 369–385, 2009.
4. Aylon Y and Oren M. Living with p53, dying of p53. *Cell* 130: 597–600, 2007.

5. Bernard C, Berthault M-F, Saulnier C, and Ktorza A. Neogenesis vs. apoptosis as main components of pancreatic ß cell mass changes in glucose-infused normal and mildly diabetic adult rats. *FASEB J* 13: 1195–1205, 1999.
6. Boucher M–J, Selander L, Carlsson L, and Edlund H. Phosphorylation marks IPF1/PDX1 protein for degradation by glycogen synthase kinase 3-dependent mechanisms. *J Biol Chem* 281: 6395–6403, 2006.
7. Carroll JS, Liu XS, Brodsky AS, Li W, Meyer CA, Szary AJ, Eeckhoute J, Shao W, Hestermann EV, Geistlinger TR, Fox EA, Silver PA, and Brown M. Chromosome-wide mapping of estrogen receptor binding reveals long-range regulation requiring the forkhead protein FoxA1. *Cell* 122: 33–43, 2005.
8. Chan CB, Saleh MC, Koshkin V, and Wheeler MB. Uncoupling protein 2 and islet function. *Diabetes* 53: S136–142, 2004.
9. Chen H, Li X, and Epstein PN. MnSOD and catalase transgenes demonstrate that protection of islets from oxidative stress does not alter cytokine toxicity. *Diabetes* 54: 1437–1446, 2005.
10. Chen X, Scholl TO, Leskiw MJ, Donaldson MR, and Stein TP. Association of glutathione peroxidase activity with insulin resistance and dietary fat intake during normal pregnancy. *J Clin Endocrinol Metab* 88: 5963–5968, 2003.
11. Docherty HM, Hay CW, Ferguson LA, Barrow J, Durward E, and Docherty K. Relative contribution of PDX-1, MafA and E47/beta2 to the regulation of the human insulin promoter. *Biochem J* 389: 813–820, 2005.
12. Dong F, Fang C, Yang X, Zhang X, Lopez F, and Ren J. Cardiac overexpression of catalase rescues cardiac contractile dysfunction induced by insulin resistance: Role of oxidative stress, protein carbonyl formation and insulin sensitivity. *Diabetologia* 49: 1421–1433, 2006.
13. Elstner E. Oxygen radicals—Biochemical basis for their efficacy. *Klin Wochenschr* 69: 949–956, 1991.
14. Esposito F, Chirico G, Gesualdi NM, Posadas I, Ammendola R, Russo T, Cirino G, and Cimino F. Protein kinase B activation by reactive oxygen species is independent of tyrosine kinase receptor phosphorylation and requires Src activity. *J Biol Chem* 278: 20828–20834, 2003.
15. Fallon M, Gorelick F, Anderson J, Mennone A, Saluja A, and Steer M. Effect of cerulein hyperstimulation on the paracellular barrier of rat exocrine pancreas. *Gastroenterology* 108: 1863–1872, 1995.
16. Gao N, LeLay J, Vatamaniuk MZ, Rieck S, Friedman JR, and Kaestner KH. Dynamic regulation of Pdx1 enhancers by Foxa1 and Foxa2 is essential for pancreas development. *Genes Dev* 15: 3435–3448, 2008.
17. Giorgio S, Linares E, Capurro ML, Bianchi AG, and Augusto O. Formation of nitrosyl hemoglobin and nitrotyrosine during murine leishmaniasis. *Photochem Photobiol* 63: 750–754, 1996.
18. Hansen LL, Ikeda Y, Olsen GS, Busch AK, and Mosthaf L. Insulin signaling is inhibited by micromolar concentrations of H2O2. Evidence for a role of H2O2 in tumor necrosis factor alpha-mediated insuli n resistance. *J Biol Chem* 274: 25078–25084, 1999.
19. Harmon JS, Stein R, and Robertson RP. Oxidative stress-mediated, post-translational loss of MafA protein as a contributing mechanism to loss of insulin gene expression in glucotoxic beta cells. *J Biol Chem* 280: 11107–11113, 2005.
20. Hashizume K, Hirasawa M, Imamura Y, Noda S, Shimizu T, Shinoda K, Kurihara T, Noda K, Ozawa Y, Ishida S, Miyake Y, Shirasawa T, and Tsubota K. Retinal dysfunction and progressive retinal cell death in Sod1-deficient mice. *Am J Pathol* 172: 1325–1331, 2008.
21. Hennige AM, Burks DJ, Ozcan U, Kulkarni RN, Ye J, Park S, Schubert M, Fisher TL, Dow MA, Leshan R, Zakaria M, Mossa–Basha M, and White MF. Upregulation of insulin receptor substrate-2 in pancreatic beta cells prevents diabetes. *J Clin Invest* 112: 1521–1532, 2003.
22. Houstis N, Rosen ED, and Lander ES. Reactive oxygen species have a causal role in multiple forms of insulin resistance. *Nature* 440: 944–948, 2006.
23. Kawamori D, Kajimoto Y, Kaneto H, Umayahara Y, Fujitani Y, Miyatsuka T, Watada H, Leibiger IB, Yamasaki Y, and Hori M. Oxidative stress induces nucleo-cytoplasmic translocation of pancreatic transcription factor Pdx-1 through activation of c-Jun NH2-terminal kinase. *Diabetes* 52: 2896–2904, 2003.
24. Kubisch H, Wang J, Bray T, and Phillips J. Targeted overexpression of Cu/Zn superoxide dismutase protects pancreatic beta-cells against oxidative stress. *Diabetes* 46: 1563–1566, 1997.
25. Kushner JA, Ye J, Schubert M, Burks DJ, Dow MA, Flint CL, Dutta S, Wright CVE, Montminy MR, and White MF. Pdx1 restores beta cell function in Irs2 knockout mice. *J Clin Invest* 109: 1193–1201, 2002.
26. Lantz KA, Vatamaniuk MZ, Brestelli JE, Friedman JR, Matschinsky FM, and Kaestner KH. Foxa2 regulates multiple pathways of insulin secretion. *J Clin Invest* 114: 512–520, 2004.
27. Lee CS, Sund NJ, Vatamaniuk MZ, Matschinsky FM, Stoffers DA, and Kaestner KH. Foxa2 controls pdx1 gene expression in pancreatic beta cells *in vivo*. *Diabetes* 51: 2546–2551, 2002.
28. Lei X, Zhu J, McClung J, Aregullin M, and Roneker C. Mice deficient in Cu,Zn-superoxide dismutase are resistant to acetaminophen toxicity. *Biochem J* 399: 455–461, 2006.
29. Lenzen S, Drinkgern J, and Tiedge M. Low antioxidant enzyme gene expression in pancreatic islets compared with various other mouse tissues. *Free Radic Biol Med* 20: 463–466, 1996.
30. Li X, Chen H, and Epstein PN. Metallothionein and catalase sensitize to diabetes in nonobese diabetic mice: Reactive oxygen species may have a protective role in pancreatic beta cells. *Diabetes* 55: 1592–1604, 2006.
31. Mahadev K, Zilbering A, Zhu L, and Goldstein BJ. Insulin-stimulated hydrogen peroxide reversibly inhibits protein-tyrosine phosphatase 1B *in vivo* and enhances the early insulin action cascade. *J Biol Chem* 276: 21938–21942, 2001.
32. Malaisse WJ and Sener A. Glucose-induced changes in cytosolic ATP content in pancreatic islets. *Bioch Biophy Acta Mol Cell Res* 927: 190–195, 1987.
33. McClung JP, Roneker CA, Mu W, Lisk DJ, Langlais P, Liu F, and Lei XG. Development of insulin resistance and obesity in mice overexpressing cellular glutathione peroxidase. *Proc Nat Acad Sci USA* 101: 8852–8857, 2004.
34. Otsuka M, Satake H, Murakami S, Doi M, Ishida T, and Shibasaki M. An artificial CuII complex with intriguing oxygen radical-quenching profile. X-ray structure, cytochrome c assay, and ESR study. *Bioorg Med Chem* 4: 1703–1708, 1996.
35. Panowski SH, Wolff S, Aguilaniu H, Durieux J, and Dillin A. PHA-4/Foxa mediates diet-restriction-induced longevity of *C. elegans*. *Nature* 447: 550–555, 2007.
36. Park J, Stoffers D, Nicholls R, and Simmons R. Development of type 2 diabetes following intrauterine growth retardation in rats is associated with progressive epigenetic silencing of Pdx1. *J Clin Invest* 118: 2316–2324, 2008.

37. Rafikova O, Salah EM, and Tofovic SP. Renal and metabolic effects of tempol in obese ZSF1 rats–distinct role for superoxide and hydrogen peroxide in diabetic renal injury. *Metabolism* 57: 1434–1444, 2008.
38. Robertson R. Chronic oxidative stress as a central mechanism for glucose toxicity in pancreatic islet beta cells in diabetes. *J Biol Chem* 279: 42351–42354, 2004.
39. Saldeen J, Lee JC, and Welsh N. Role of p38 mitogen-activated protein kinase (p38 MAPK) in cytokine-induced rat islet cell apoptosis. *Biochem Pharmacol* 61: 1561–1569, 2001.
40. Sanfey H, Bulkley G, and Cameron J. The role of oxygen-derived free radicals in the pathogenesis of acute pancreatitis. *Ann Surg* 200: 405–413, 1984.
41. Schoenberg M, Birk D, and Beger H. Oxidative stress in acute and chronic pancreatitis. *Am J Clin Nutr* 62: 1306S–1314, 1995.
42. Stoffers D. The development of beta-cell mass: Recent progress and potential role of Glp-1. *Horm Metab Res* 36: 811–821, 2004.
43. Stoffers DA, Stanojevic V, and Habener JF. Insulin promoter factor-1 gene mutation linked to early-onset type 2 diabetes mellitus directs expression of a dominant negative isoprotein. *J Clin Invest* 102: 232–241, 1998.
44. Tanaka Y, Tran POT, Harmon J, and Robertson RP. A role for glutathione peroxidase in protecting pancreatic beta cells against oxidative stress in a model of glucose toxicity. *Proc Nat Acad Sci USA* 99: 12363–12368, 2002.
45. Thorens B, Guillam M-T, Beermann F, Burcelin R, and Jaquet M. Transgenic reexpression of Glut1 or Glut2 in pancreatic beta cells rescues Glut2-null mice from early death and restores normal glucose-stimulated insulin secretion. *J Biol Chem* 275: 23751–23758, 2000.
46. Tiedge M, Lortz S, Drinkgern J, and Lenzen S. Relation between antioxidant enzyme gene expression and antioxidative defense status of insulin-producing cells. *Diabetes* 46: 1733–1742, 1997.
47. Wang X, Gillen EA, van der Meulen Marjolein CH, and Lei XG. Knockouts of Se-glutathione peroxidase-1 and Cu,Zn superoxide dismutase exert different impacts on femoral mechanical performance of growing mice. *Mol Nutr Food Res* 52: 1334–1339, 2008.
48. Wang XD, Vatamaniuk MZ, Wang SK, Roneker CA, Simmons RA, and Lei XG. Molecular mechanisms for hyperinsulinaemia induced by overproduction of selenium-dependent glutathione peroxidase-1 in mice. *Diabetologia* 51: 1515–1524, 2008.
49. Zhang C–Y, Baffy G, Perret P, Krauss S, Peroni O, Grujic D, Hagen T, Vidal–Puig AJ, Boss O, and Kim Y–B. Uncoupling protein-2 negatively regulates insulin secretion and is a major link between obesity, beta cell dysfunction, and type 2 diabetes. *Cell* 105: 745–755, 2001.
50. Zhu J–H, Zhang X, Roneker CA, McClung JP, Zhang S, Thannhauser TW, Ripoll DR, Sun Q, and Lei XG. Role of copper,zinc-superoxide dismutase in catalyzing nitrotyrosine formation in murine liver. *Free Radic Biol Med* 45: 611–618, 2008.

Address correspondence to:
X.G. Lei, Ph.D.
252 Morrison Hall
Cornell University
Ithaca, NY 14853

E-mail: XL20@cornell.edu

Date of first submission to ARS Central, May 26, 2010; date of acceptance, June 27, 2010.

Abbreviations Used

AKT = protein kinase B
ChIP = chromatin immunoprecipitation
CuDIPS = copper diisopropylsalicylate
DETC = diethyldithiocarbamate
DKO = double knockout of glutathione peroxidase 1 and superoxide dismutase 1
Foxa2 = forkhead box A2
GPX1 = glutathione peroxidase 1
GSIS = glucose-stimulated insulin secretion
GTT = glucose tolerance test
H3 = histone 3
H3K4 = histone 3 lysine 4
HO/XO = hypoxanthine/xanthine oxidase
IR = insulin receptor
IRS-1 = insulin receptor substrate-1
ITT = insulin tolerance test
JNK = c-jun terminal kinase
Pdx1 = pancreatic and duodenal homeobox 1
ROS = reactive oxygen species
SOD1 = superoxide dismutase 1
Ucp2 = uncoupled protein 2
WT = wild-type

This article has been cited by:

1. Li Wang, Zongyong Jiang, Xin Gen Lei. 2012. Knockout of SOD1 alters murine hepatic glycolysis, gluconeogenesis, and lipogenesis. *Free Radical Biology and Medicine* **53**:9, 1689-1696. [CrossRef]
2. Xiaoping Sun, Toshimitsu Komatsu, Jinhwan Lim, Mara Laslo, Jason Yolitz, Cecilia Wang, Luc Poirier, Thomas Alberico, Sige Zou. 2012. Nutrient-dependent requirement for SOD1 in lifespan extension by protein restriction in Drosophila melanogaster. *Aging Cell* **11**:5, 783-793. [CrossRef]
3. Min-Shu Zeng, Xi Li, Yan Liu, Hua Zhao, Ji-Chang Zhou, Ke Li, Jia-Qiang Huang, Lv-Hui Sun, Jia-Yong Tang, Xin-Jie Xia, Kang-Ning Wang, Xin Gen Lei. 2012. A high-selenium diet induces insulin resistance in gestating rats and their offspring. *Free Radical Biology and Medicine* **52**:8, 1335-1342. [CrossRef]
4. JennaLynn Styskal, Holly Van Remmen, Arlan Richardson, Adam B. Salmon. 2012. Oxidative stress and diabetes: What can we learn about insulin resistance from antioxidant mutant mouse models?. *Free Radical Biology and Medicine* **52**:1, 46-58. [CrossRef]
5. Ning Li, Suzana Stojanovski, Pierre Maechler. 2012. Mitochondrial Hormesis in Pancreatic # Cells: Does Uncoupling Protein 2 Play a Role?. *Oxidative Medicine and Cellular Longevity* **2012**, 1-9. [CrossRef]
6. John W. Finley, Ah-Ng Kong, Korry J. Hintze, Elizabeth H. Jeffery, Li Li Ji, Xin Gen Lei. 2011. Antioxidants in Foods: State of the Science Important to the Food Industry. *Journal of Agricultural and Food Chemistry* **59**:13, 6837-6846. [CrossRef]
7. Shi Kui Wang, Jeremy D. Weaver, Sheng Zhang, Xin Gen Lei. 2011. Knockout of SOD1 promotes conversion of selenocysteine to dehydroalanine in murine hepatic GPX1 protein. *Free Radical Biology and Medicine* **51**:1, 197-204. [CrossRef]
8. Xin Gen Lei , Marko Z. Vatamaniuk . 2011. Two Tales of Antioxidant Enzymes on # Cells and Diabetes. *Antioxidants & Redox Signaling* **14**:3, 489-503. [Abstract] [Full Text HTML] [Full Text PDF] [Full Text PDF with Links]